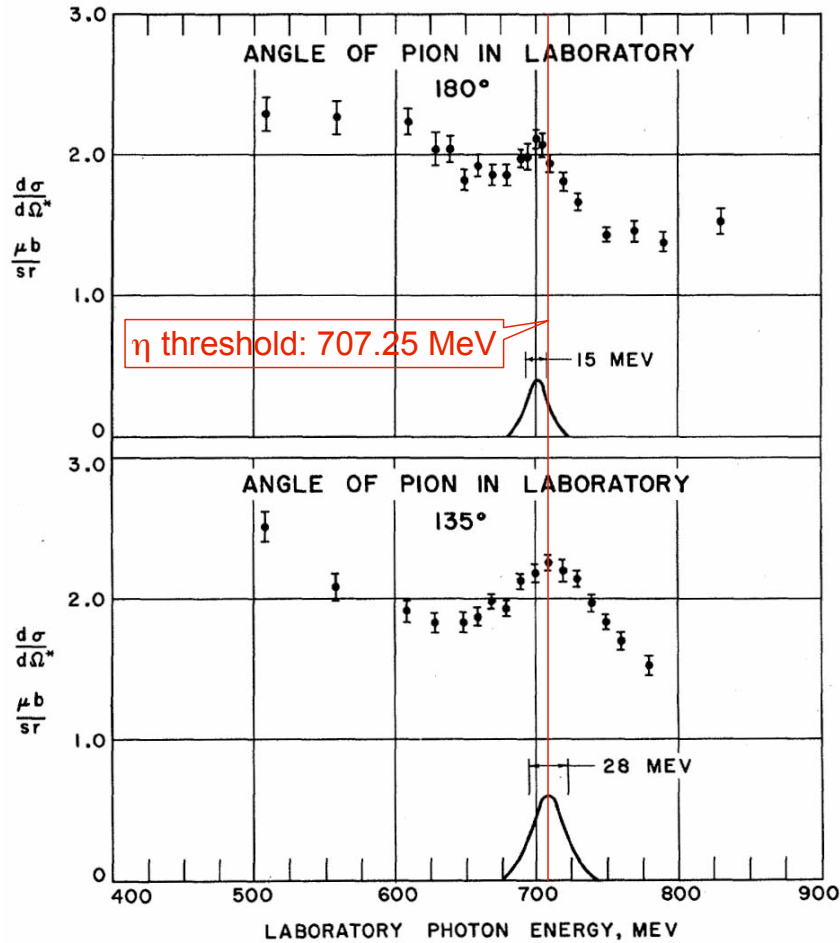


Narrow Resonances
in
Meson Photoproduction

Carlo Schaerf
for the
Graal Collaboration

University of Rome "Tor Vergata"
and
INFN - Sezione di Roma Tor Vergata

$\rho(\gamma, \pi^+)n$ at 180°



Pion Photoproduction at Backward Angles Near the Second Nucleon-Pion Resonance,
L. Hand and C. Schaerf
PRL 6, 229 (1961)

FIG. 1. Differential cross section in the center-of-mass system as a function of photon energy at fixed laboratory angles of the pion. The solid lines indicate the photon energy resolution as calculated from the spectrometer momentum acceptance, the angular variation of the kinematics, and the finite target size.

$p(\gamma, \pi^+)n$ at 180°

3'2. *Experimental results.* - The results of this experiment are summarized in Table I and illustrated in Fig. 4. The assigned errors indicate only statistical fluctuations.

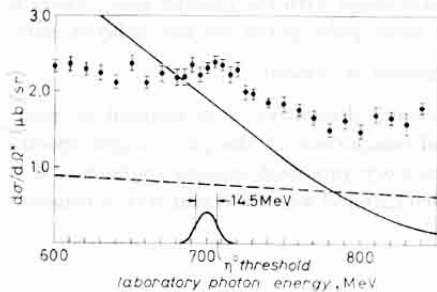


Fig. 4. - Excitation curve at a pion angle of 180° . The solid curve indicates the results of the analysis of SALIN (ref. ⁽⁹⁾). The broken line indicates the result of the theoretical calculations of HÖHLER and SCHMIDT (ref. ⁽⁹⁾).

TABLE I. - Center-of-mass differential cross-section in microbarn/steradian as a function of the gamma-ray energy K .

K (MeV)	$d\sigma/d\Omega$ ($\mu\text{b}/\text{sr}$)	K (MeV)	$d\sigma/d\Omega$ ($\mu\text{b}/\text{sr}$)
600	2.23 ± 0.084	715	2.02 ± 0.107
610	2.24 ± 0.115	720	2.18 ± 0.113
620	2.07 ± 0.081	725	1.83 ± 0.105
630	2.29 ± 0.123	730	1.82 ± 0.104
640	1.85 ± 0.110	740	1.60 ± 0.068
650	2.12 ± 0.113	750	1.60 ± 0.099
660	1.92 ± 0.076	760	1.73 ± 0.089
670	1.94 ± 0.107	770	1.61 ± 0.097
680	2.00 ± 0.105	780	1.45 ± 0.095
685	2.10 ± 0.107	790	1.62 ± 0.099
690	2.17 ± 0.116	810	1.85 ± 0.151
695	2.14 ± 0.116	820	1.66 ± 0.077
700	2.10 ± 0.063	830	1.45 ± 0.106
705	2.21 ± 0.078	840	1.65 ± 0.075
710	2.16 ± 0.073		

Positive Pion Photoproduction at 180° Near the Second Nucleon-Pion Resonance

C. Schaerf

Il Nuovo Cimento 44A, 504 (1966)

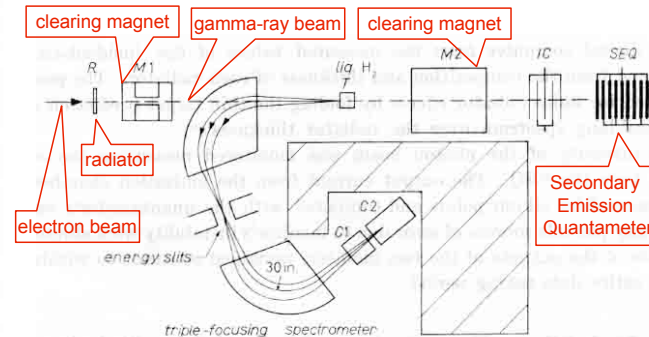


Fig. 1. - Diagram of experimental layout (see text).

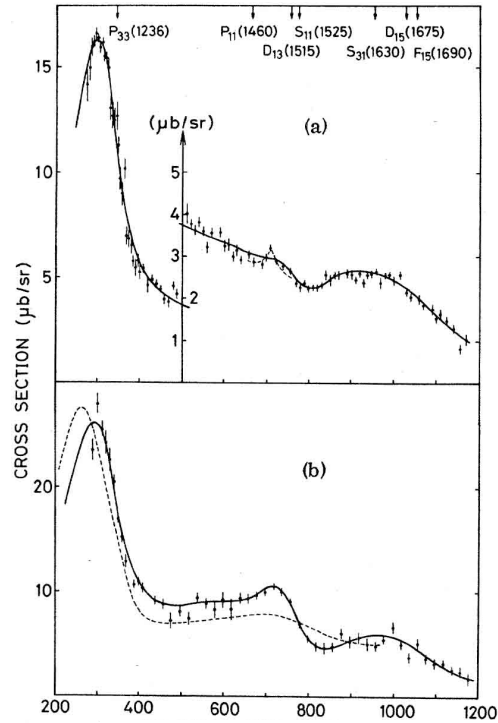


FIG. 1. Differential cross sections at 180° as functions of photon energy (a) for $\gamma + p \rightarrow \pi^+ + n$, and (b) for $\gamma + n \rightarrow \pi^+ + p$. The solid curves are the resonance-model fits. The dashed line in (a) is a result of the multichannel analysis for a cusp effect. The dashed line in (b) is calculated with the amplitudes of Walker's analysis.

PRL 26, 1672 (1971)

$\rho(\gamma, \pi^+)n$ at 180°

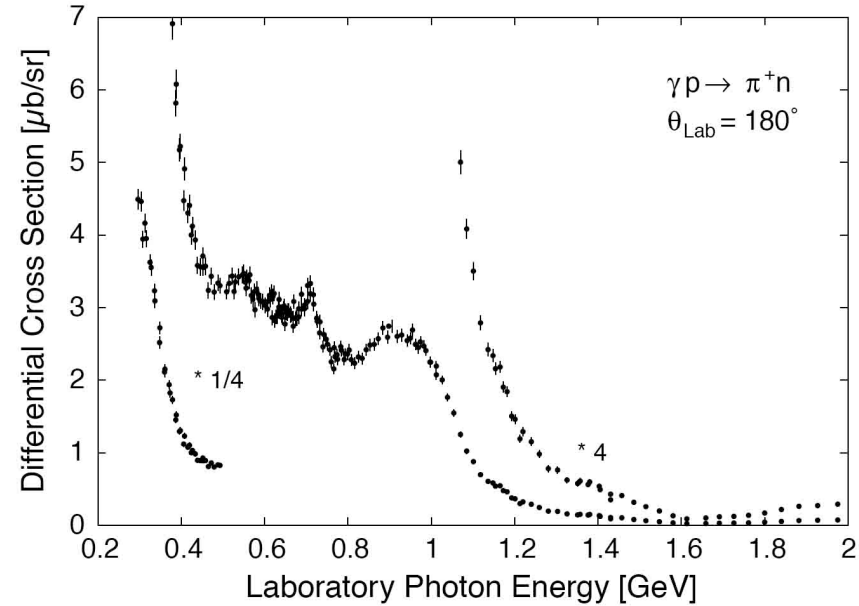
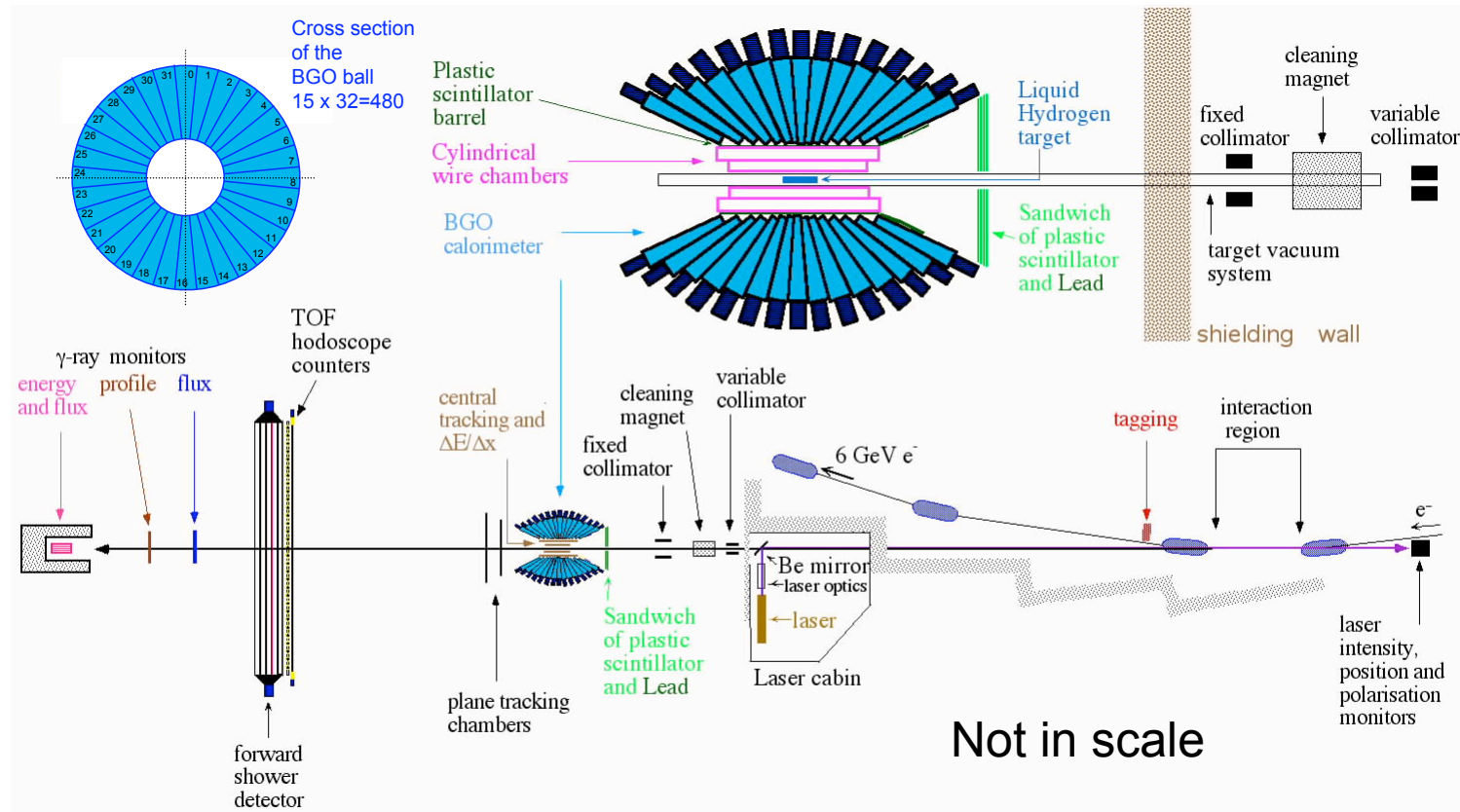


Fig. 9. Differential cross-section for $\gamma p \rightarrow \pi^+ n$ at a laboratory pion angle of $\theta = 180^\circ$ as a function of the laboratory photon energy. The data around the first resonance are reduced to $1/4$ and above the third resonance the cross-sections are in addition plotted after multiplication by 4.

EPJ A 11, 441 (2001)

The Graal Apparatus



The Graal Detector

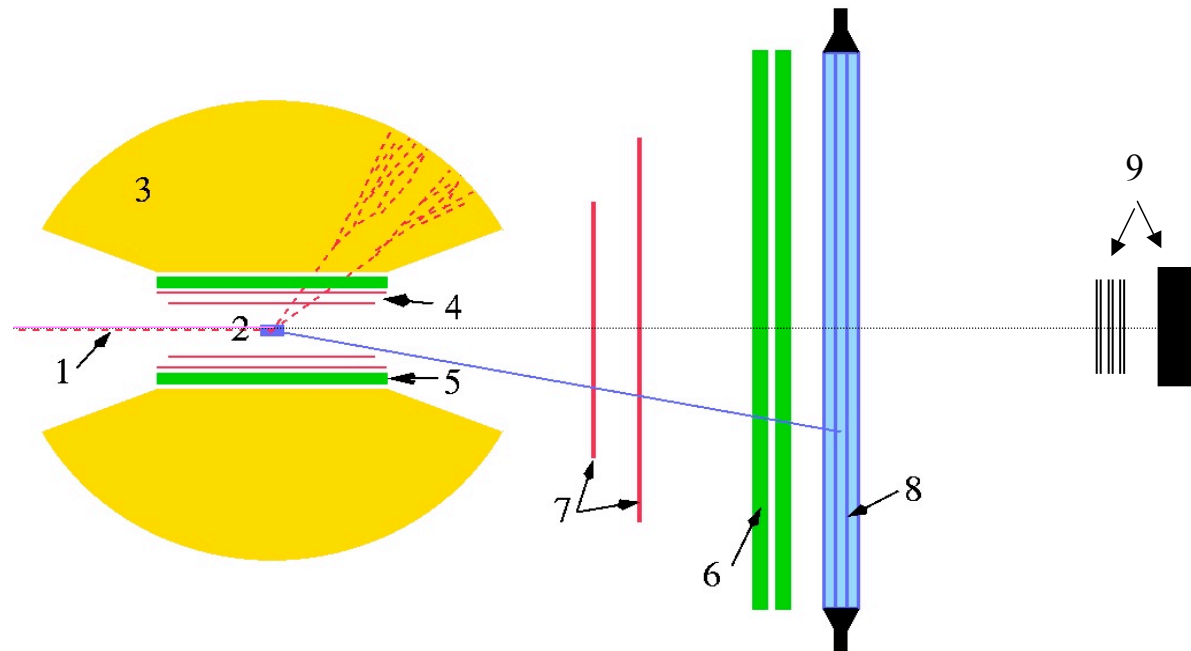
➤ Liquid Target :
2 H² or D²

➤ Central angles :
 $25^\circ < \theta < 155^\circ$

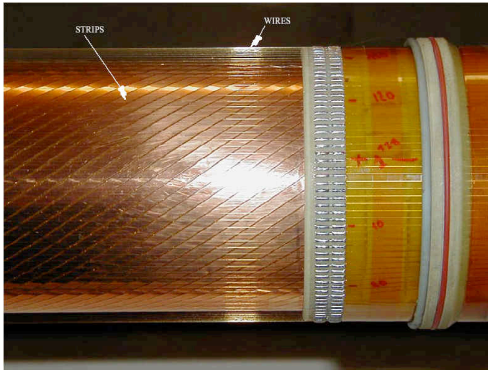
➤ Forward angles :
 $\theta < 25^\circ$

- BGO calorimeter
- 2 cylindrical MWPC
- barrel of plastic scintillators

- 6 double wall of scintillators
- 7 planar MWPC
- 8 shower wall
- 9 monitor detectors



Central Angles ($25^\circ < \theta < 155^\circ$): MWPC, BARREL



- **2 cylindrical MWPC**

tracking of the charged particles

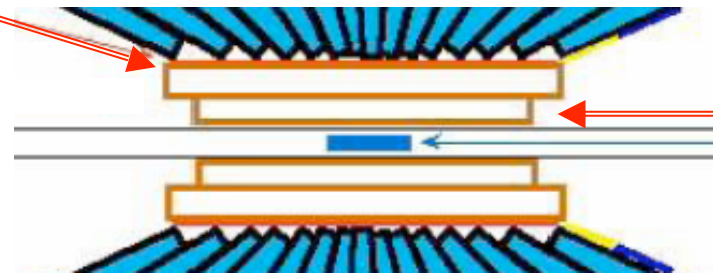
Angular resolution $\Delta\theta = 2^\circ$
 $\Delta\phi = 1.4^\circ$

Around the MWPC:

- **barrel of 32 plastic scintillators (NE102A)**



charged/neutral particles
discrimination
(veto for neutral particle)
charged particles identification
by means of dE/dx vs. E
(E is measured in the BGO)



Forward Angles ($\theta < 25^\circ$): MWPC, Hodoscope

- 2 sets of planar MWPC (xy, uv)

tracking of the charged particles

Angular resolution

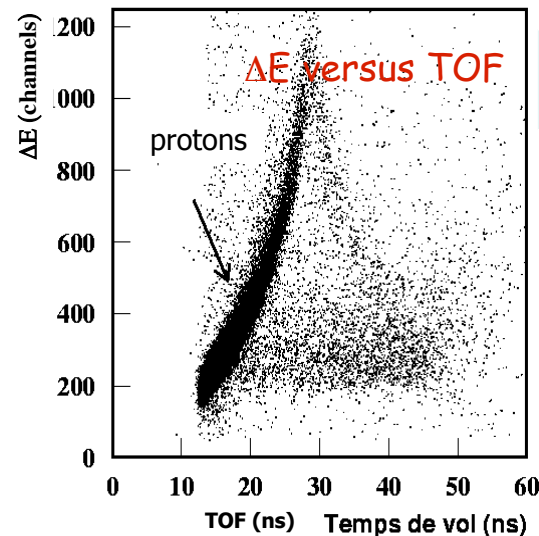
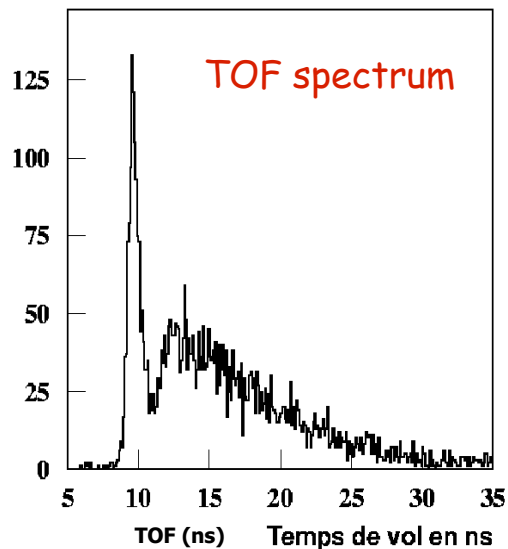
$$\Delta\theta = 2^\circ$$

$$\Delta\phi = 1.4^\circ$$

- Double Forward Scintillator Wall (hodoscope)

26 x 26 bars NE110A
300 x 11,5 x 3 mm

- Charged particle identification (pions, proton) by means ΔE vs. TOF
- TOF measurement for energy determination of charged particles



Angular resolution

$$\Delta\theta \cong \Delta\varphi \cong 3^\circ$$

Forward Angles ($\theta < 25^\circ$): Shower Wall

• Forward Shower Wall

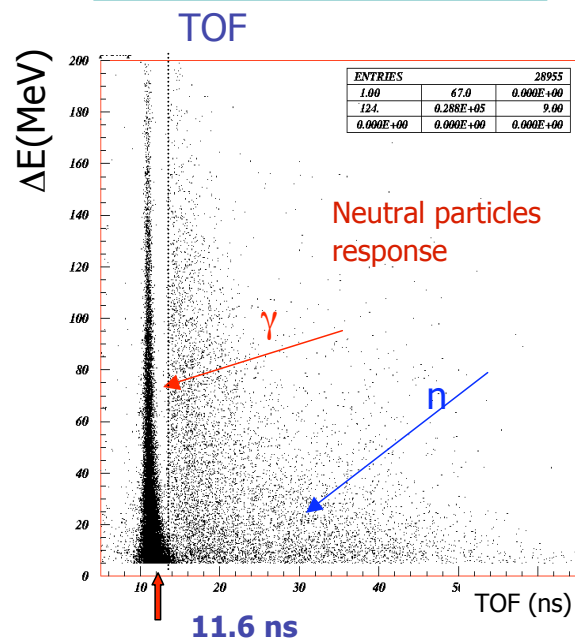
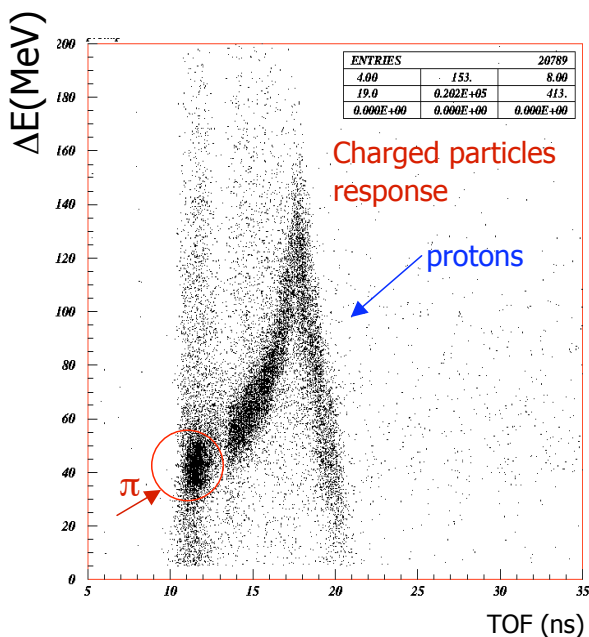
TOF measurements provide:

- ✓ Energy information for protons and neutrons
- ✓ photon/neutron discrimination
- ✓ pion/proton discrimination
- ✓ charged/neutral particle discrimination in coincidence with the hodoscope

16 *sandwich* modules :

- 4 layers of scintillators 10 cm thick
- 3 layers of lead converters 3 mm thick
- frontal iron plate 5 mm thick

photon efficiency 92-95%
neutron efficiency 22%



7/14/09

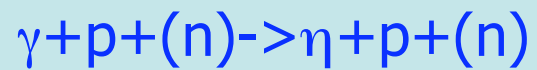
Carlo Schaerf - Edinburgh 090608

9

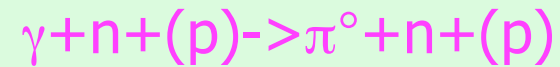
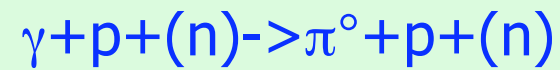
Two Examples of Meson Photoproduction

η photo-production on quasi-free nucleons from Deuteron

π^0 photo-production on quasi-free nucleons from Deuteron



➤ η photo-production
on quasi free proton
on quasi free neutron

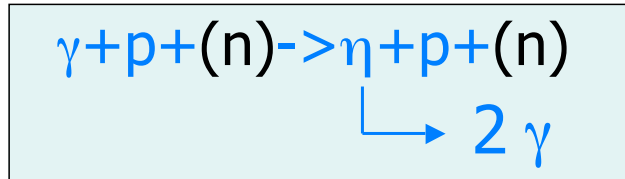


➤ π^0 photo-production
on quasi free proton
on quasi free neutron

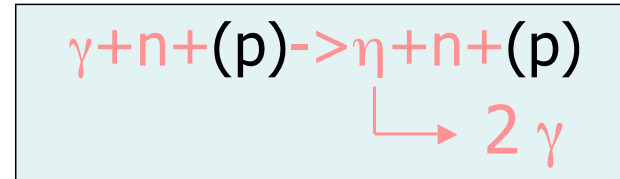
Events Selection for η Photoproduction on Quasi-Free Nucleons from Deuteron

η photo-production on quasi free proton

η photo-production on quasi free neutron



Neutron is a spectator



Proton is a spectator

2 γ in the BGO
+
participant nucleon in the central or forward direction

NO other particle
(the spectator particle is not detected)

Bi-Dimensional Cuts

Over-determined Information provided by apparatus

Particles energy and angles can be Measured or calculated by the Variables of the other particles from two-body kinematics

$$\left. \begin{array}{l} E_{\bar{\gamma}} \\ E_{\eta}^{meas} \quad \theta_{\eta}^{meas} \quad \varphi_{\eta}^{meas} \\ \theta_N^{meas} \quad \varphi_N^{meas} \end{array} \right\} \rightarrow \begin{array}{l} \theta_N^{calc} \\ E_{\eta}^{calc} \\ M_{\eta}^{miss} \end{array}$$

Bi-dimensional distributions

Each Distribution fitted by Bi-dimensional Gaussian

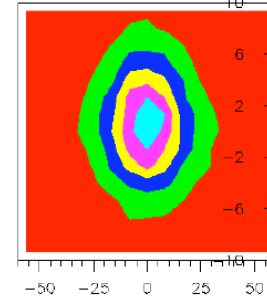
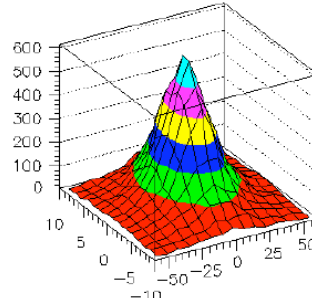
extraction of mean and σ_i values

Bi-dimensional cuts

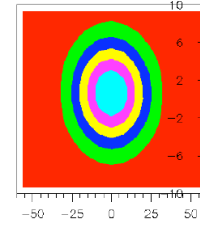
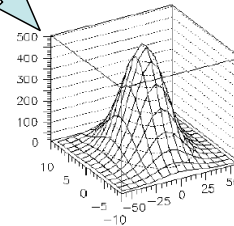
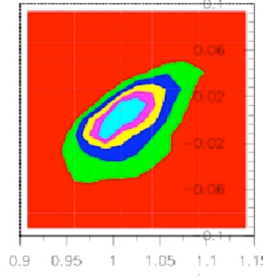
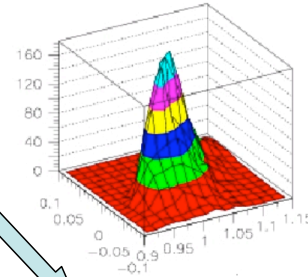
$$\frac{(x - \mu_1)^2}{\sigma_1^2} + \frac{(x - \mu_2)^2}{\sigma_2^2} - \frac{2C(x - \mu_1)(x - \mu_2)}{\sigma_1\sigma_2} < \sigma^2 \quad [\sigma = 1 - 3]$$

Selection cuts:

$$(\theta_N^{meas} - \theta_N^{calc}) \text{ vs } (\varphi_N^{meas} - \varphi_{\eta}^{meas} - 180^\circ)$$



$$(E_{\eta}^{calc} / E_{\eta}^{meas}) \text{ vs } (M_{\eta}^{miss} - M_N)$$



Events Selection – Quasi Two-Body Kinematics

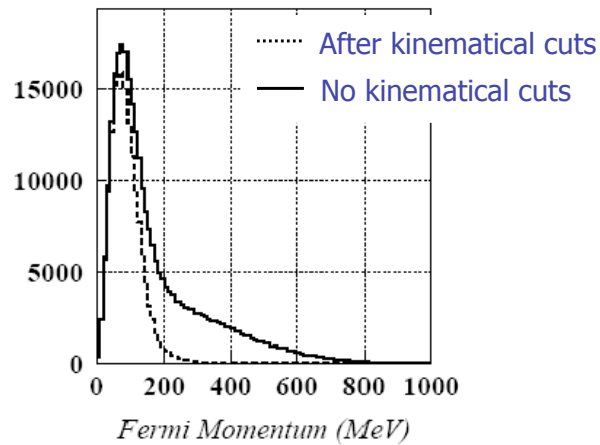
Quasi-free process
and low Fermi momentum



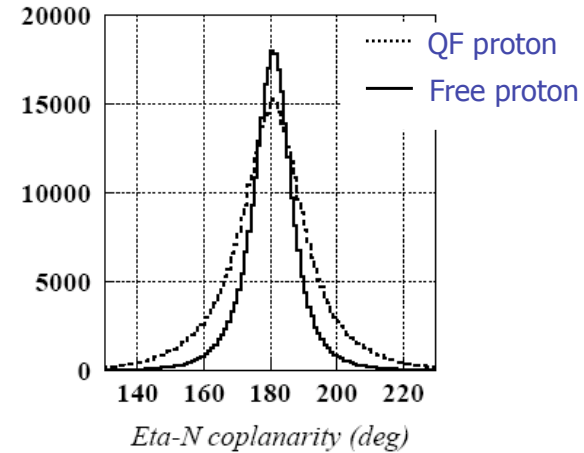
Kinematical Analysis:

- Two-body nature of each reaction step:

Fermi momentum Contribution



Smearing of distributions



η Invariant Mass and Estimated Background

a) Central proton

2.4 %

b) Central neutron

3.9 %

c) Forward proton

0.9 %

d) Forward neutron

1.4 %

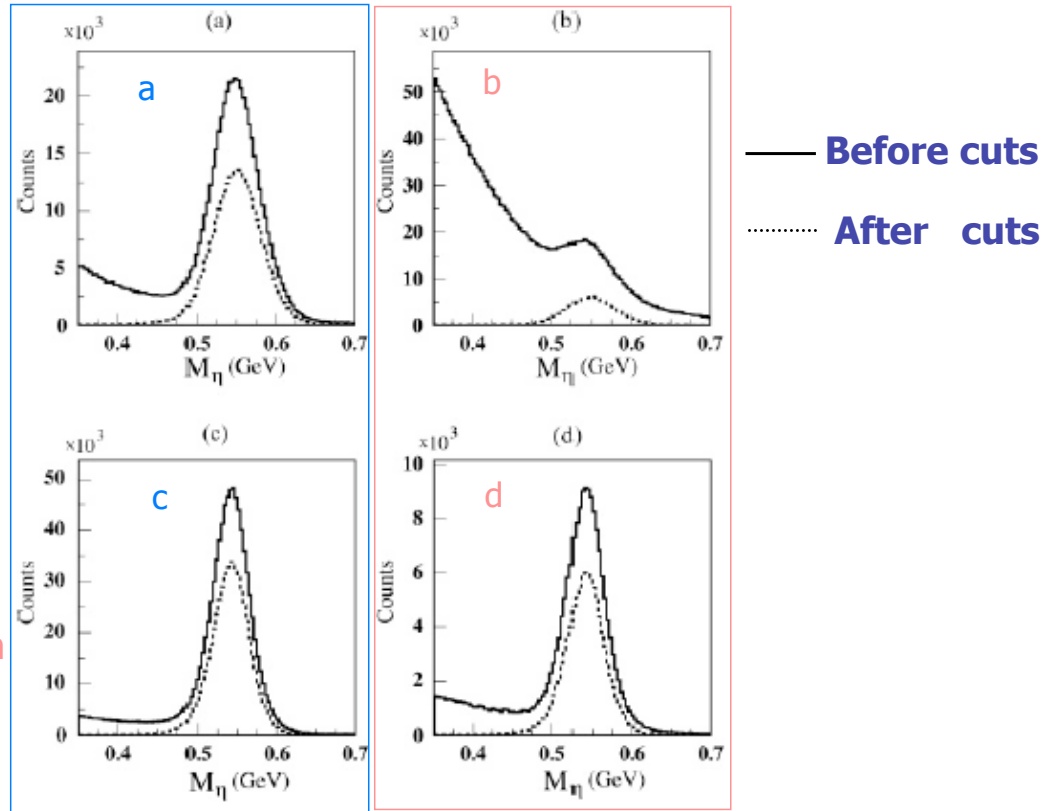
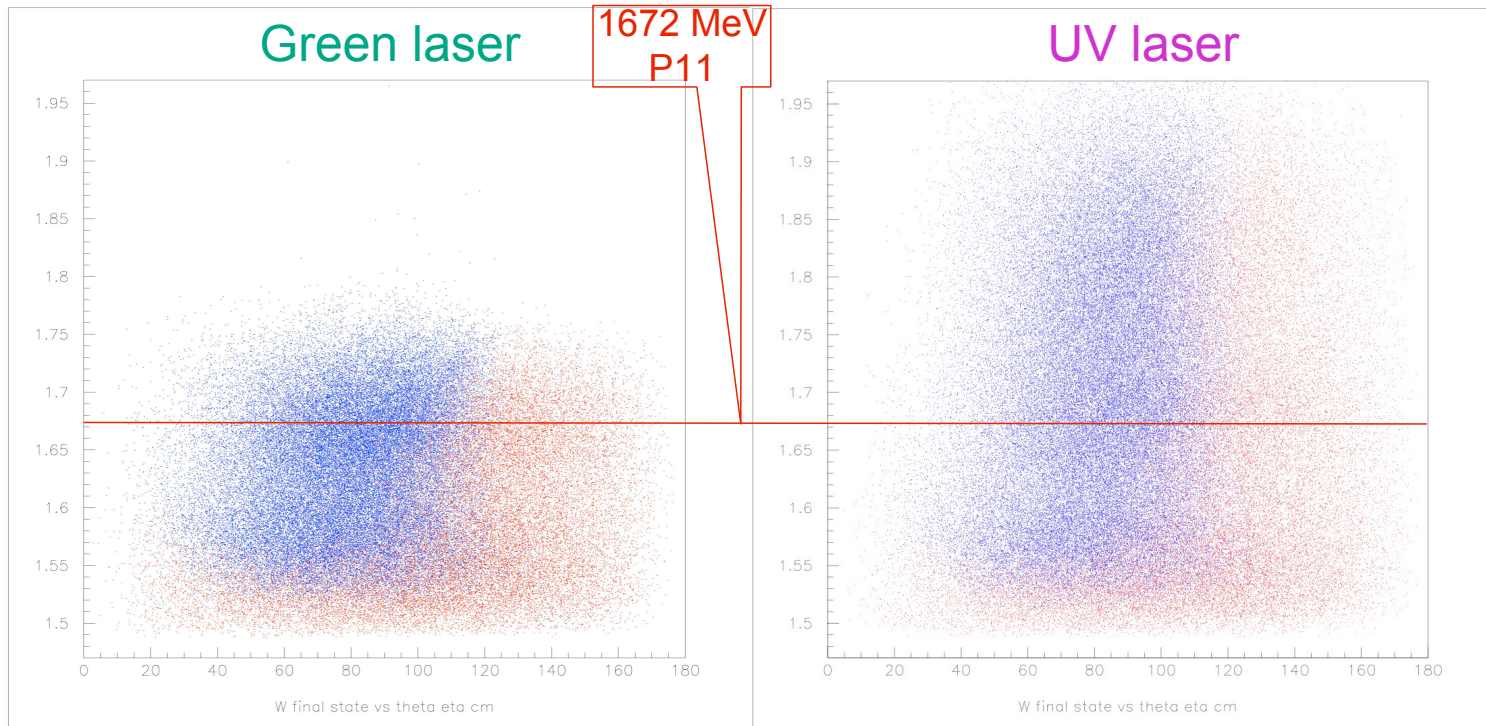


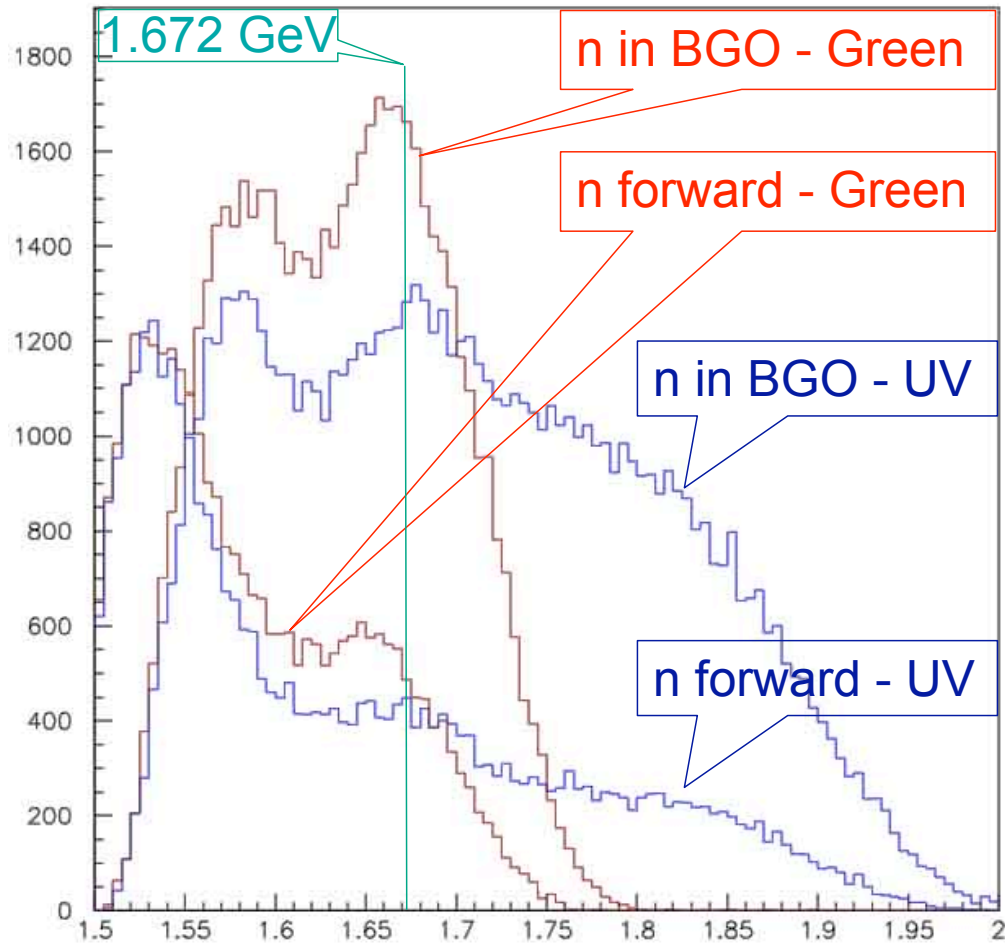
FIG. 4. The η invariant mass without cuts (solid line) and with the kinematical cuts (dotted line) for (a) a proton and (b) a neutron in the central region and for (c) a proton and (d) a neutron in the forward direction.

$w(\text{fin})$ vs $\theta_{\eta}^{\text{cm}}$



red neutron forward
blue neutron in BGO

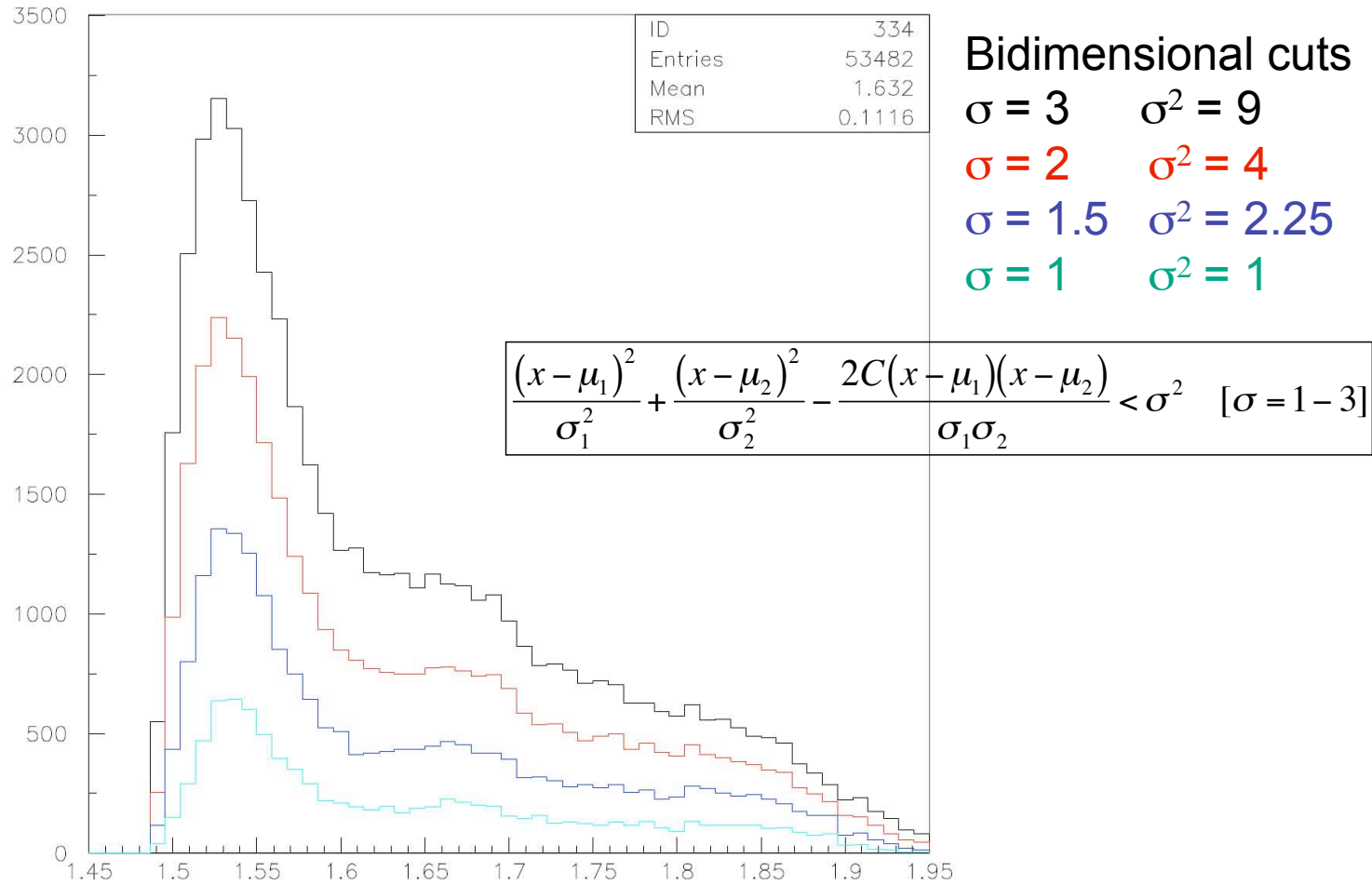
GREEN vs UV & Forward vs BGO



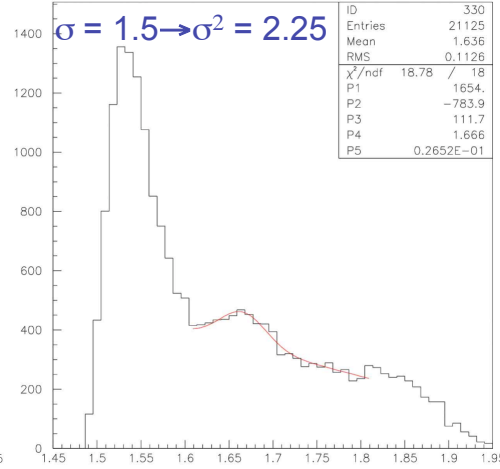
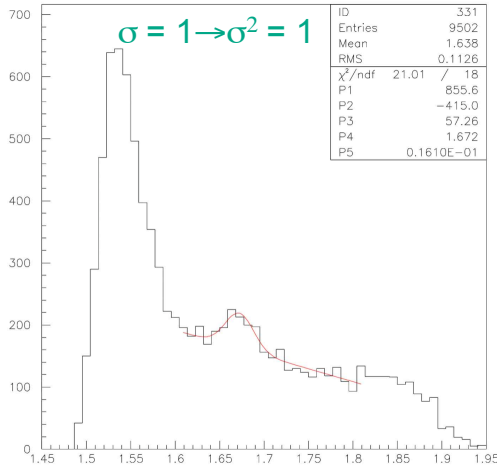
7/14/09

Carlo Schaerf - Edinburgh 090608

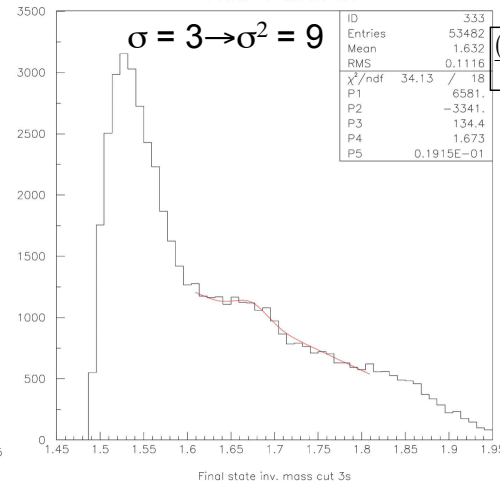
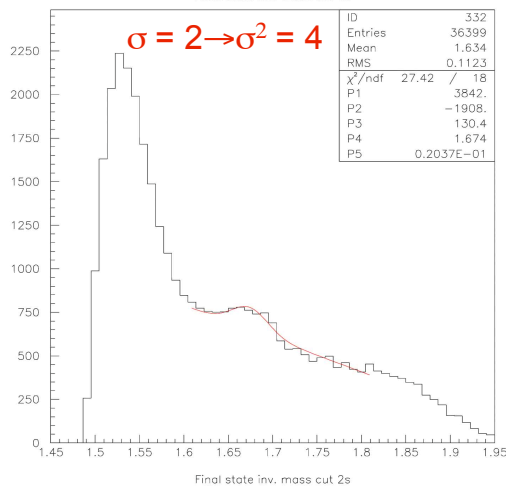
Yield vs sigma: Forward n



Resonance Width as a Function of Sigma: Forward n UV

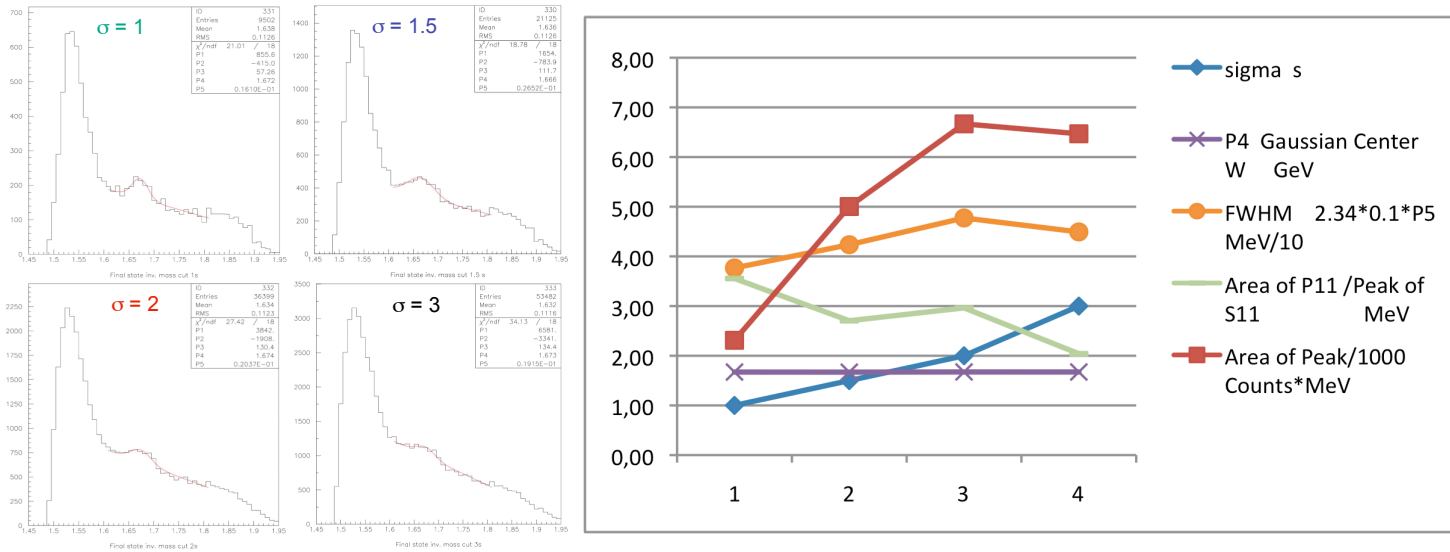


Linear fit + Gaussian:
 P3 = gaussian height
 P4 = gaussian center
 P5 = gaussian width (rms)
 Resonance position:
 $W = P4$
 Resonance width (FWHM):
 $D = 2,34 \cdot P5$
 Resonance Strenght:
 $A = P3 \cdot P5$



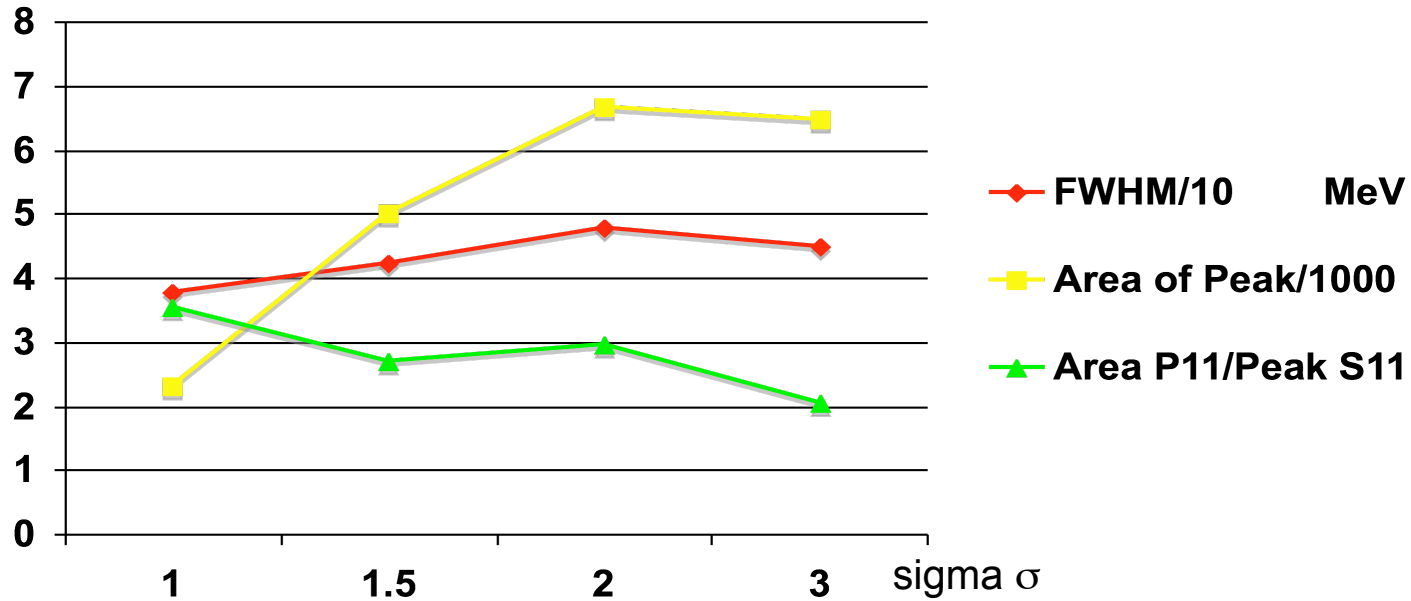
$$\frac{(x-\mu_1)^2}{\sigma_1^2} + \frac{(x-\mu_2)^2}{\sigma_2^2} - \frac{2C(x-\mu_1)(x-\mu_2)}{\sigma_1\sigma_2} < \sigma^2 \quad [\sigma = 1-3]$$

Resonance Width as a Function of Sigma: Forward n UV



sigma σ	1,00	1,50	2,00	3,00	
σ^2	1,00	2,25	4,00	9,00	
P3 P11 Gaussian Height	Counts	57,26	110,30	130,40	134,40
P4 P11 Gaussian Center	W GeV	1,672	1,670	1,674	1,673
P5 P11 Gaussian Width (rms)	MeV	16,10	18,10	20,40	19,20
P11 FWHM 2.34*0.1*P5	MeV/10	3,77	4,24	4,77	4,49
Area of P11 peak *	Counts*MeV	2310,80	5004,25	6667,96	6468,23
Peak of S11	Counts	650,00	1850,00	2250,00	3170,00
Area of P11/Peak of S11	MeV	3,56	2,71	2,96	2,04
Area of P11 Peak /1000	Counts*MeV	2,31	5,00	6,67	6,47
* Area of P11 peak= $(2\pi)^{1/2} * P5 * P3$					

Resonance Width as a Function of Sigma: Forward n UV

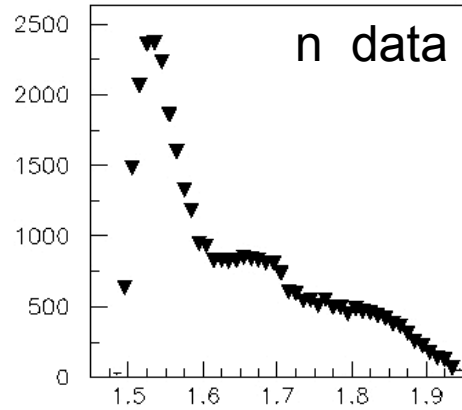


σ	σ^2	P3 Gaussian Height Counts	P4 Gaussian Center W GeV	P5 Gaussian Width (rms) MeV	$\Gamma \approx \text{FWHM}$ $2.36 * 0.1 * P5$ MeV/10	Area of peak = $(2\pi)^{1/2} * P5 * P3$ Counts*MeV	S11 Peak Counts	Area of P11 /Peak of S11 MeV	Area of Peak/1000 Counts*MeV
1,00	1,00	57,26	1,672	16,10	3,77	2310,80	650,00	3,56	2,31
1,50	2,25	110,30	1,670	18,10	4,24	5004,25	1850,00	2,71	5,00
2,00	4,00	130,40	1,674	20,40	4,77	6667,96	2250,00	2,96	6,67
3,00	9,00	134,40	1,673	19,20	4,49	6468,23	3170,00	2,04	6,47

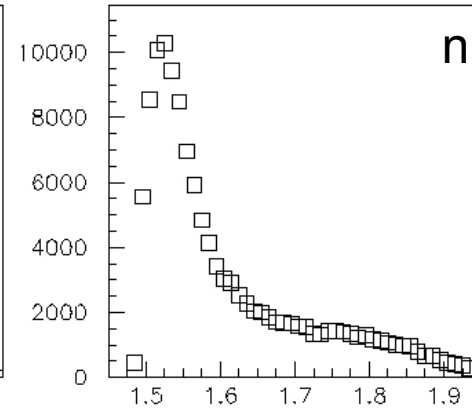
$$W = 1672 \text{ MeV} \Rightarrow k = 1018 \text{ MeV}$$

η -n Yield for all angles – Forward neutron – $\theta_{n\text{Lab}} < 25^\circ$

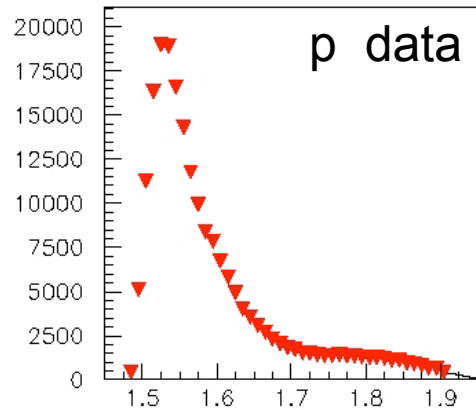
all theta eta cm angles



w eta-n final state data (GeV)

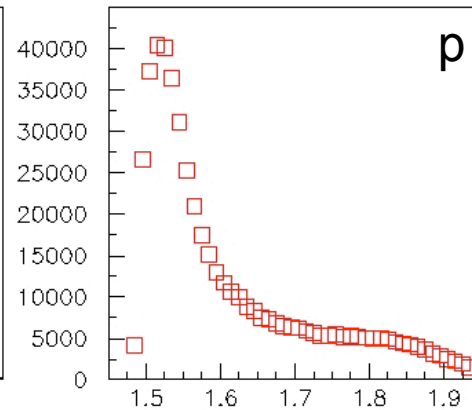


w eta-n final state sim (GeV)



w eta-p final state data (GeV)

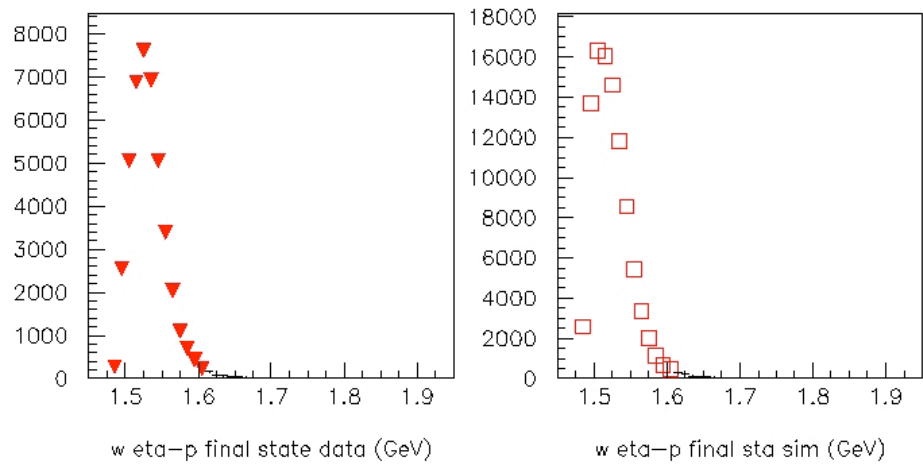
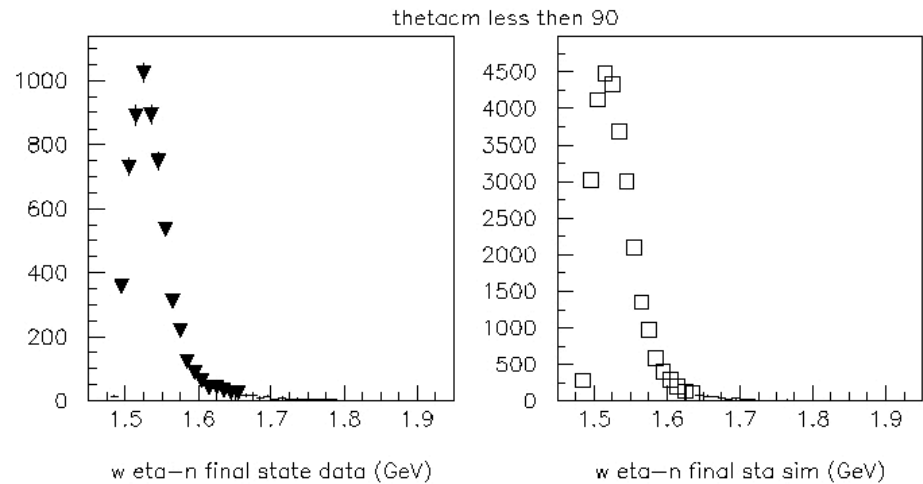
7/14/09



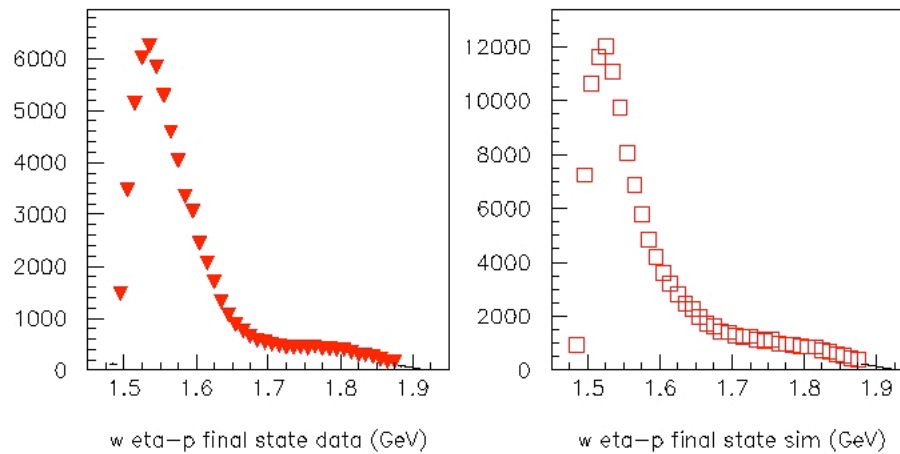
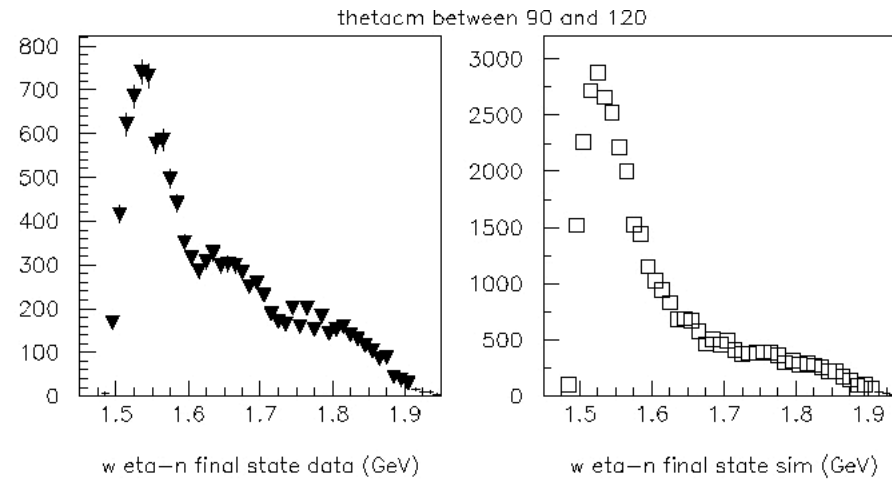
w eta-p final state sim (GeV)

Carlo Schaerf - Edinburgh 090608

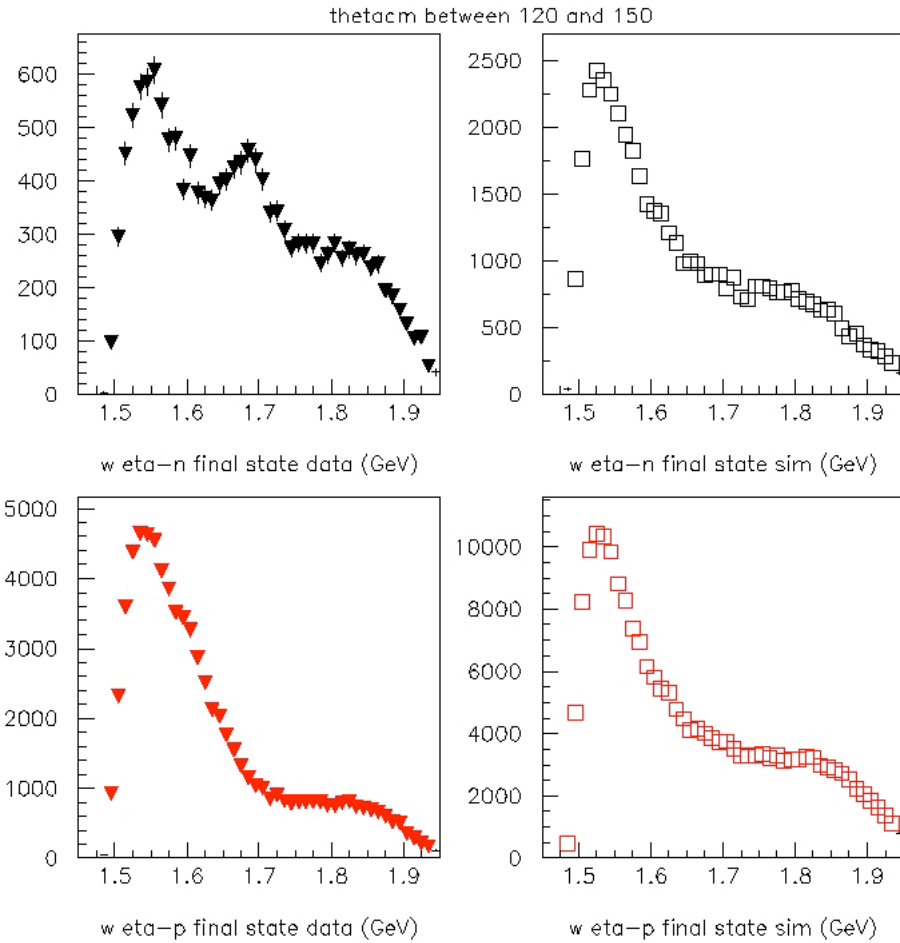
η -n Yield for $\theta_\eta < 90^\circ$



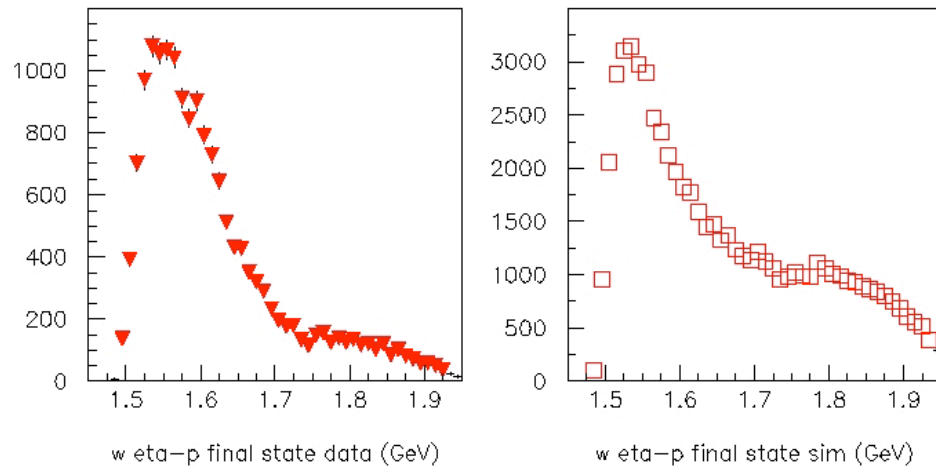
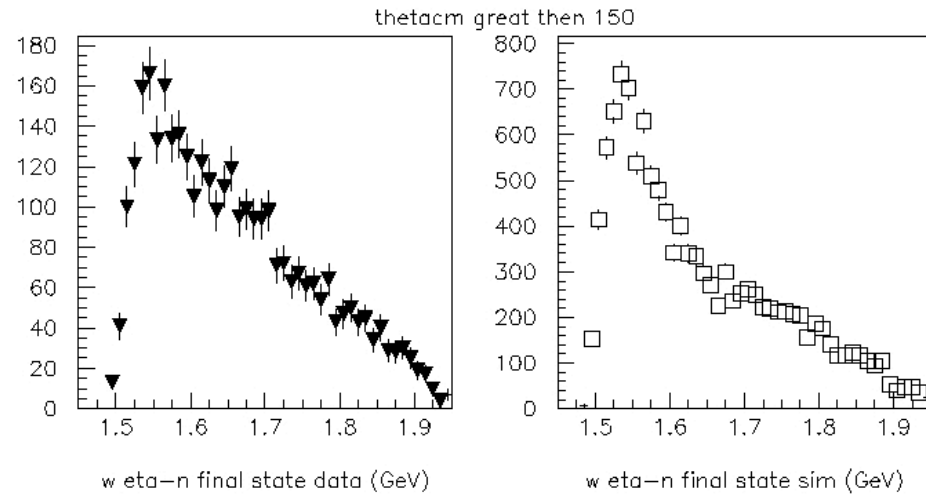
η -n Yield for $\theta_\eta = 90^\circ - 120^\circ$



η -n Yield for $\theta_\eta = 120^\circ - 150^\circ$



η -n Yield for $\theta_\eta > 150^\circ$



7/14/09

Carlo Schaerf - Edinburgh 090608

THE BEAM ASYMMETRY

Selected events grouped in
Fixed E_γ , θ_η^{cm} , ϕ_η^{cm} bins

11 E_γ bins
16 ϕ_η^{cm} bins
8 θ_η^{cm} bins

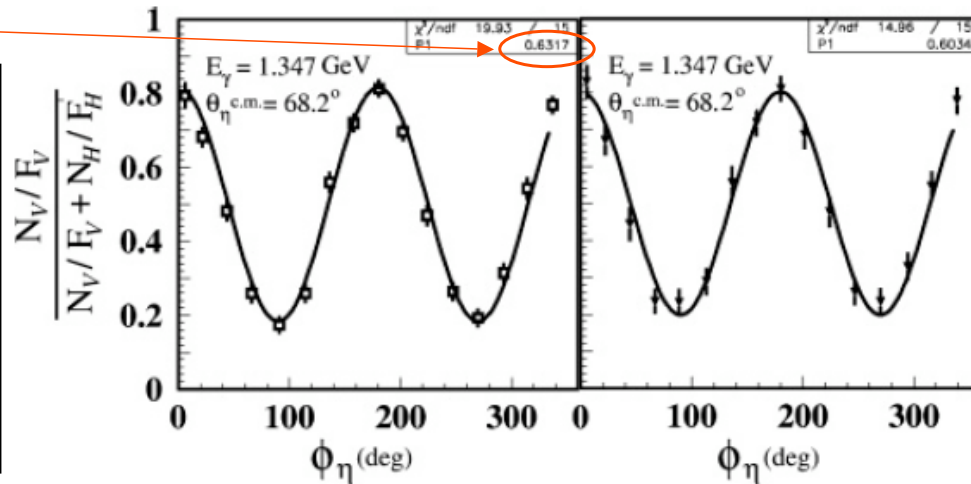
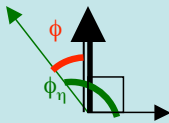
$P\Sigma$
free parameter in the fit

For each $(E_\gamma, \theta_\eta^{\text{cm}}) \Rightarrow$ Fit of azimuthal
behavior of the ratio:

$$\frac{N_V / K_V}{N_V / K_V + N_H / K_H} = \frac{1}{2} \left[1 + P \Sigma \cos(2\phi_\eta) \right]$$

$N_{V,H}$ = Number of selected events with vertical/horizontal beam polarization
 $K_{V,H}$ = Flux corresponding to vertical/horizontal beam polarization
 P = Polarization degree of the beam at the bin mean energy
 Σ = Beam asymmetry to be determined for every $(E_\gamma, \theta_\eta^{\text{cm}})$

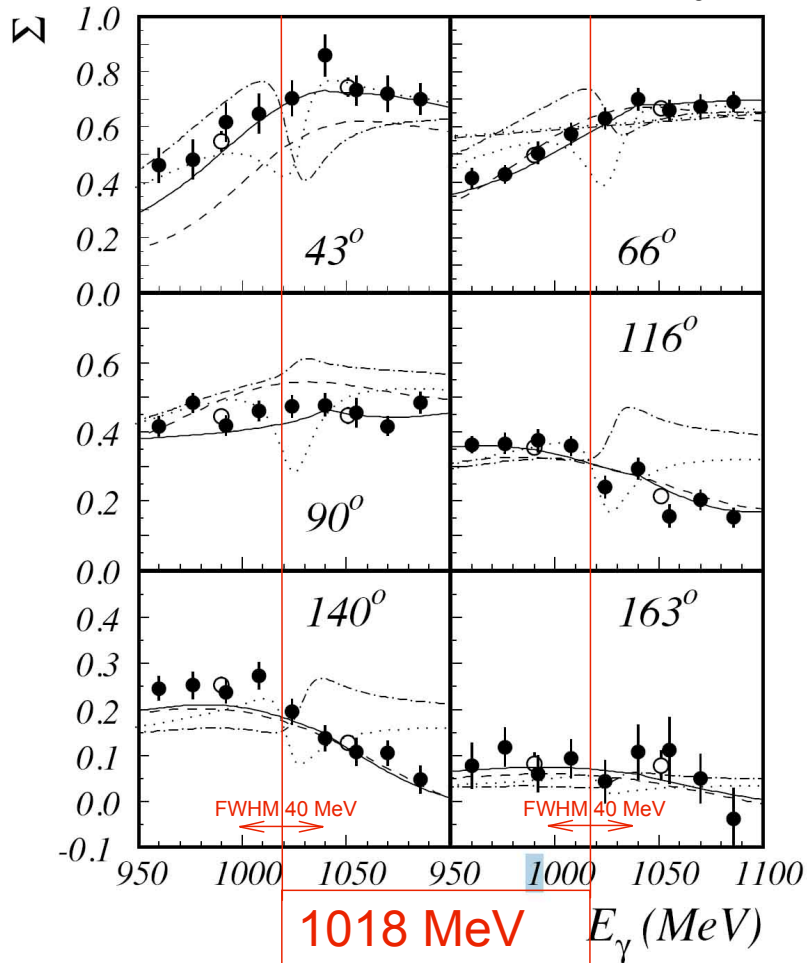
NB:
The + sign in front of $P\Sigma\cos(2\phi_\eta)$ term in the distribution is due to the coordinate system choice.
If ϕ is the angle between the reaction plan and the polarization direction of the photon and ϕ_η is the azimuthal angle of outgoing meson, we have:



QF-PROTON DATA

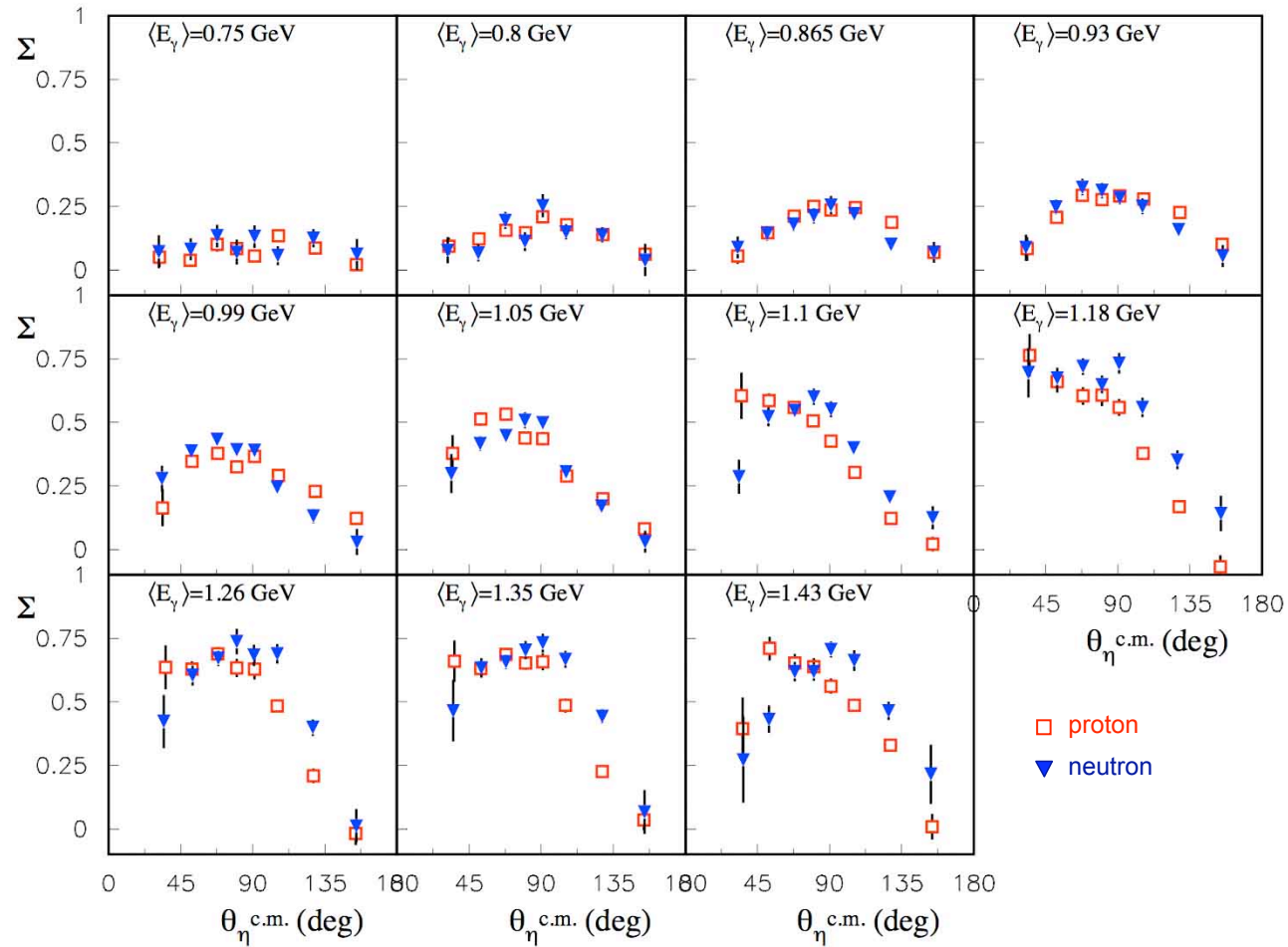
QF-NEUTRON DATA

Asimmetry Σ free p

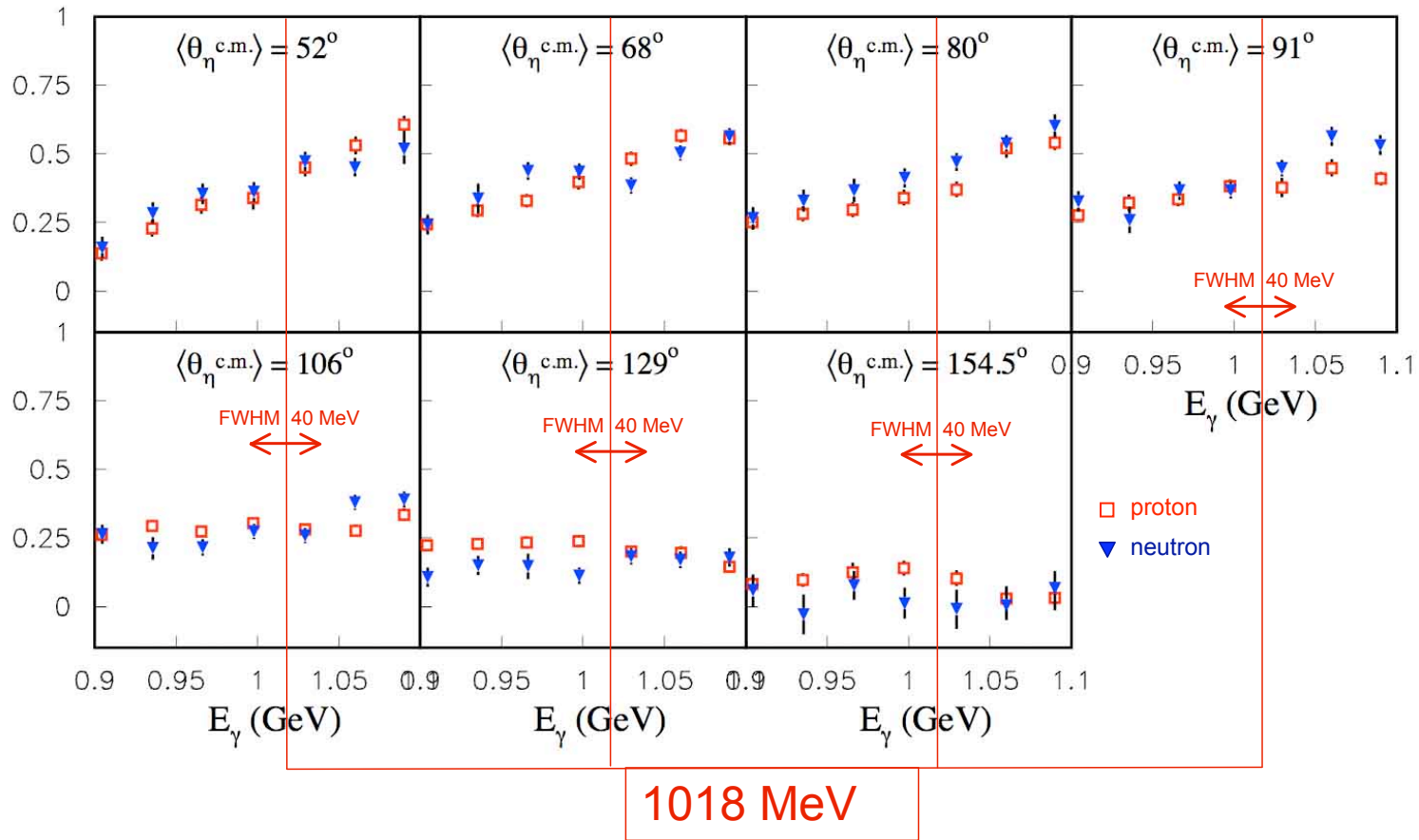


Asymmetry between 950 and 1100 MeV obtained with a narrow energy binning for various η center-of-mass angles. Comparison with the standard MAID model (dashed line), BCC partial-wave analysis (solid line) and predictions of the modified reggeized MAID model including a narrow P11 state. For this latter model, two versions are displayed corresponding to the two choices for the $\zeta_{\eta N}$ hadronic relative phase (dot-dashed line: $\zeta_{\eta N}=+1$, dotted line: $\zeta_{\eta N}=-1$).

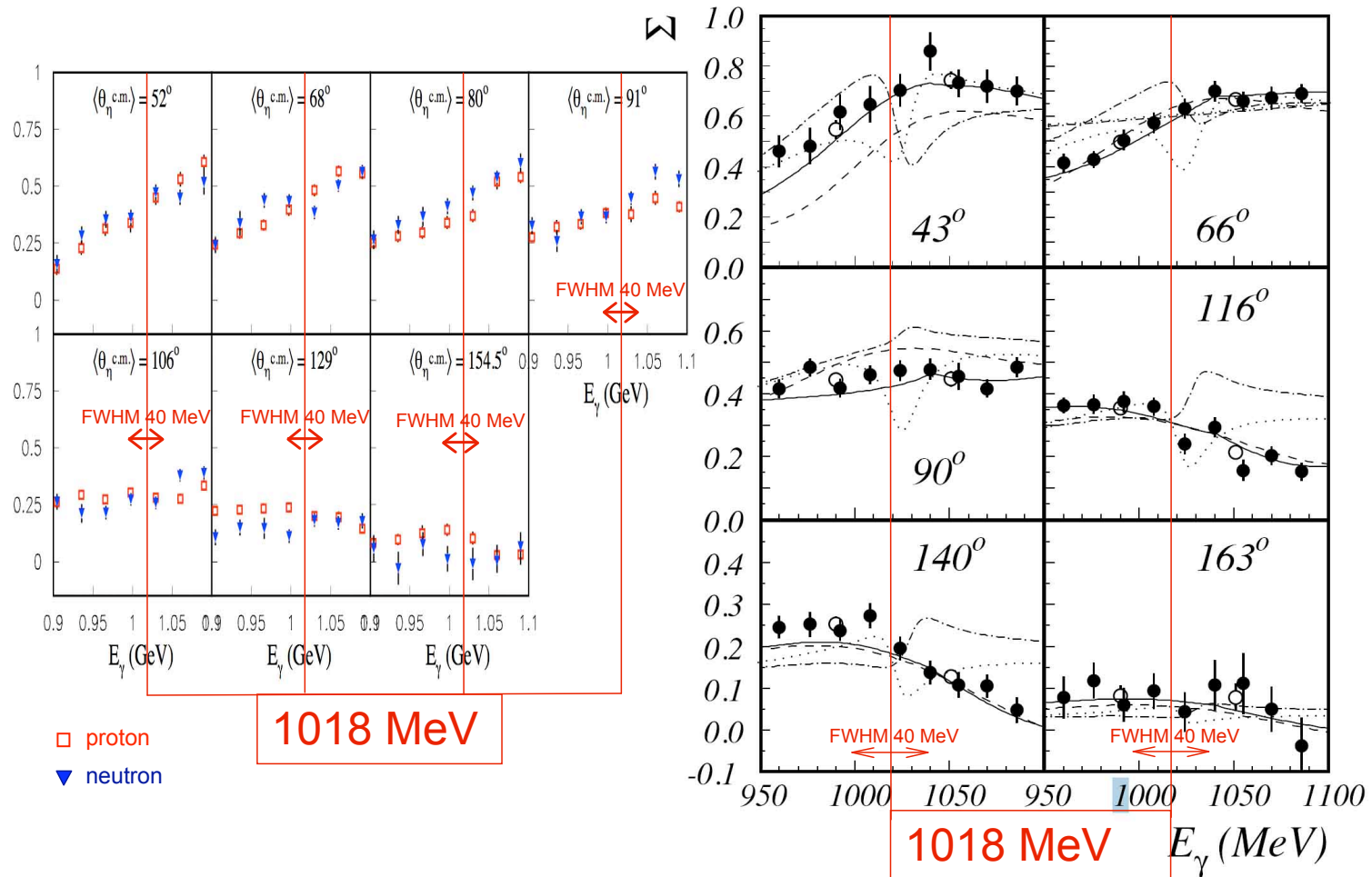
Asimmetry Σ quasi-free p vs n



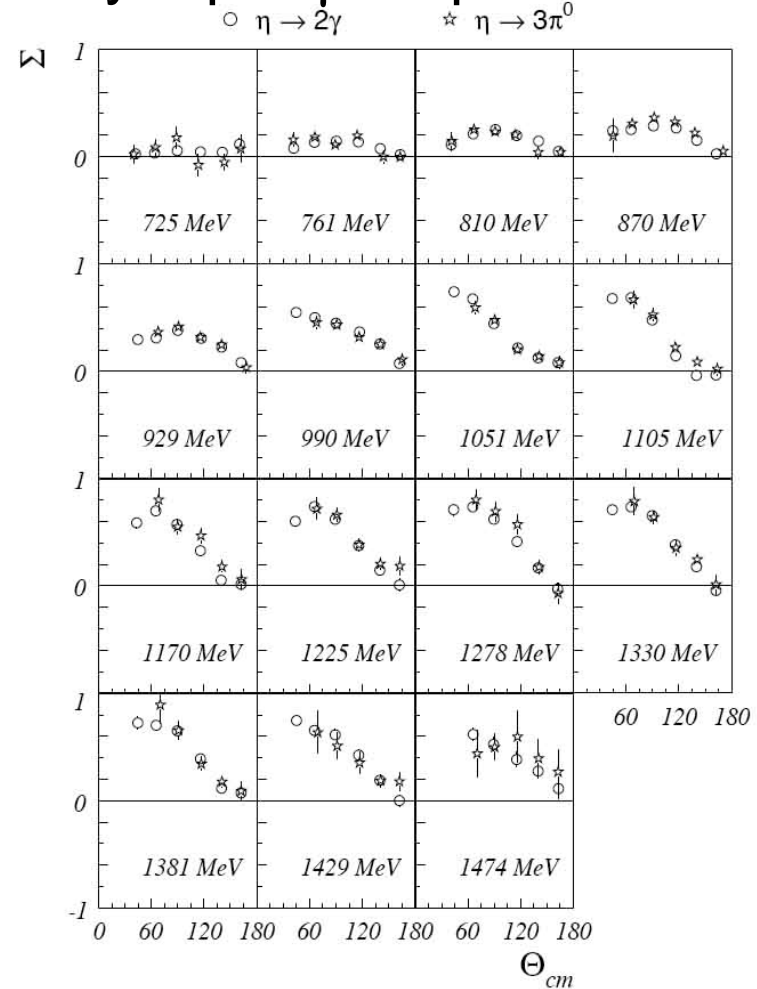
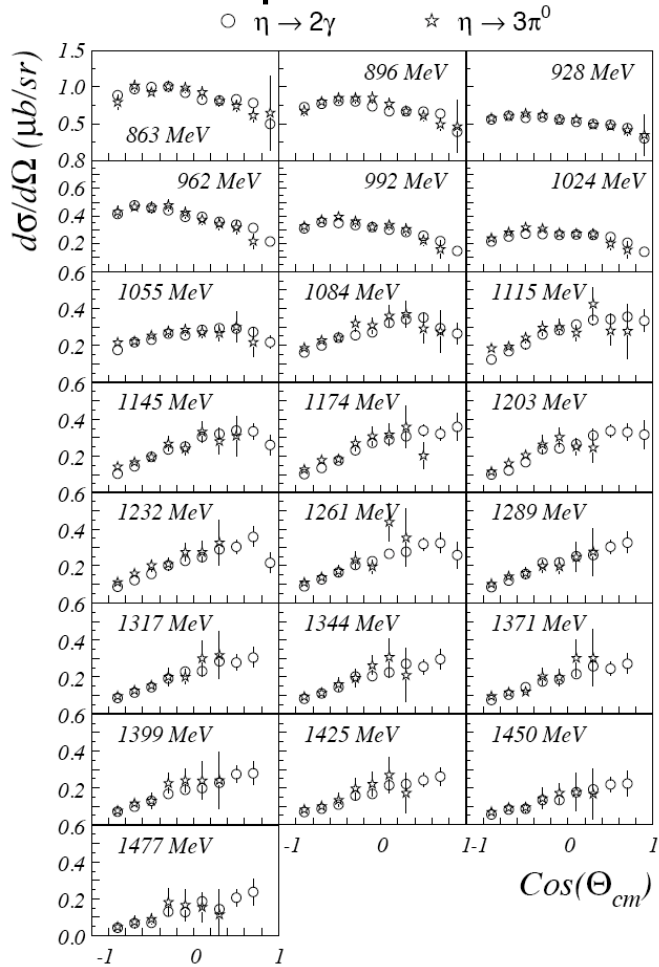
Asimmetry Σ quasi-free p vs n



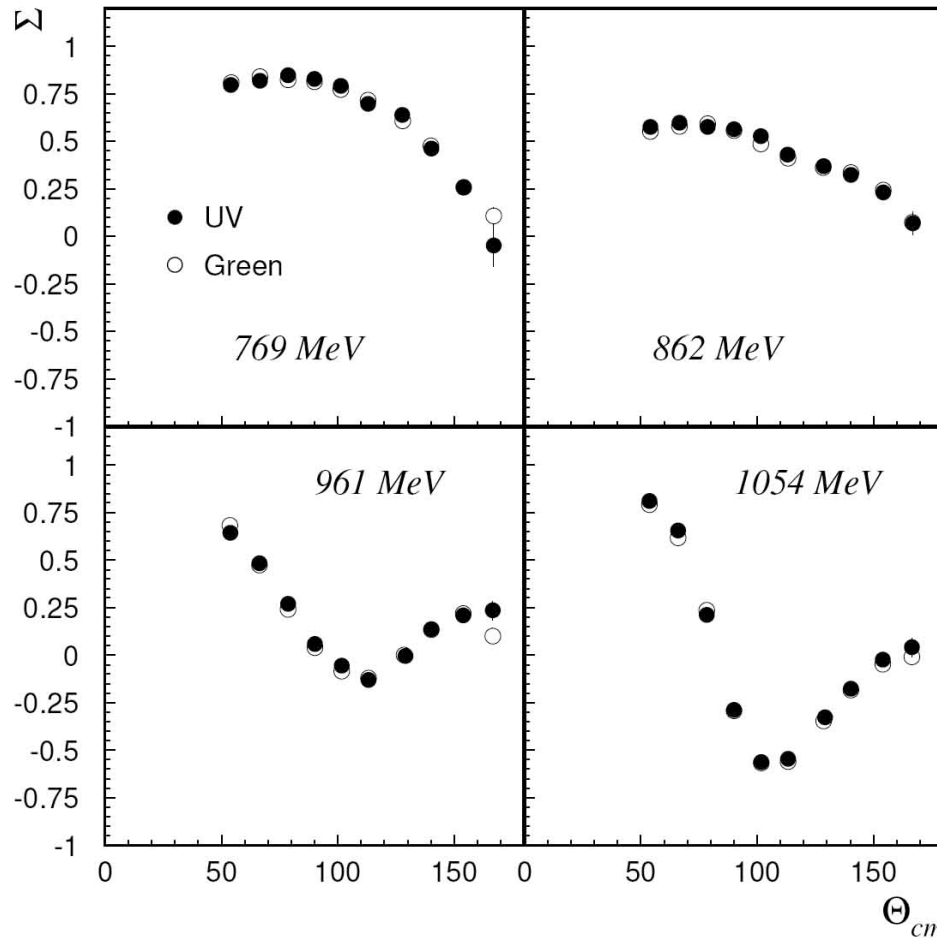
Asimmetry Σ quasi-free p/n and free p



Free p - $d\sigma/d\Omega$ + Asimmetry - $\eta \rightarrow 2\gamma$ vs $\eta \rightarrow 3\pi^0$



Asimmetry $\Sigma \pi^0$ Green vs UV



The asymmetry obtained with the Green laser line versus the UV is shown for the $\gamma + p \rightarrow p + \pi^0$ reaction which has a large cross section.